

Investigation of gas fuelling characteristics in JET experiments

A. Salmi¹, R. Gomes², J. Harrison³, A. Järvinen⁴, L. Meneses², S. Mordijk⁵, V. Naulin⁶, J. Juul Rasmussen⁶, T. Tala¹, A. Thrysoe⁶, A. Wynn⁷, E. Belonohy^{3,8}, A. Loarte⁹, M. Maslov³, M. Romanelli³, A.C.C. Sips^{8,10}, M. Tsalas⁹ and JET contributors*

EUROfusion Consortium, JET, Culham Science Centre, Abingdon, OX14 3DB, UK

¹VTT, Espoo, Finland; ²IPFN, IST, Universidade de Lisboa, Portugal; ³CCFE, Abingdon, UK;

⁴LLNL, Livermore, USA; ⁵College of William & Mary, Virginia, USA; ⁶DTU Physics, Lyngby, Denmark; ⁷York Plasma Institute, University of York, UK; ⁸JET Exploitation Unit, Culham, UK;

⁹ITER Organization, France; ¹⁰European Commission, Brussels, Belgium;

Experiments scanning pedestal transparency to study plasma-fuelling processes have been carried out on the JET tokamak in Culham, UK. All the plasmas feature also gas fuelling modulations and strike point sweepings both in deuterium and in hydrogen for inducing periodic particle source perturbations whose effects could be seen in a multitude of measured quantities, from Langmuir probes to radiation and in particular in electron density. Figure 2 shows the overview of discharges in this dataset. The plasmas are mainly type-I ELM My H-modes but feature also L-modes and type-III ELM regimes. One can observe a strong correlation between the pedestal density and ELM frequency even in the rather mixed set of discharges with total heating ranging between 5-23MW.

Note that, e.g. the heating also affects the ELM frequency. The same dependency as seen in the averaged data (Figure 1, bottom right frame): ELM frequency increases with density when $ne_{ped} > 3e19 m^{-3}$ and decreases with density

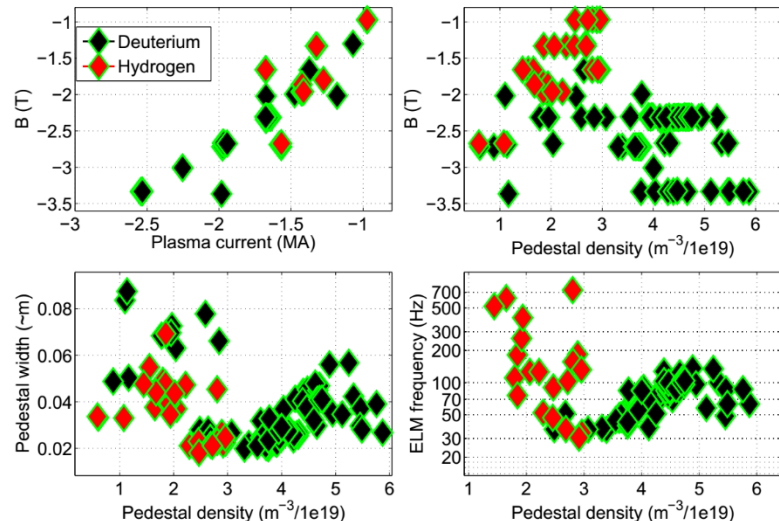


Figure 2 Parameter ranges scanned within the modulation experiments. ELM frequencies and pedestal parameters are averaged over the long quasi-stationary periods (typically ~ 5 s).

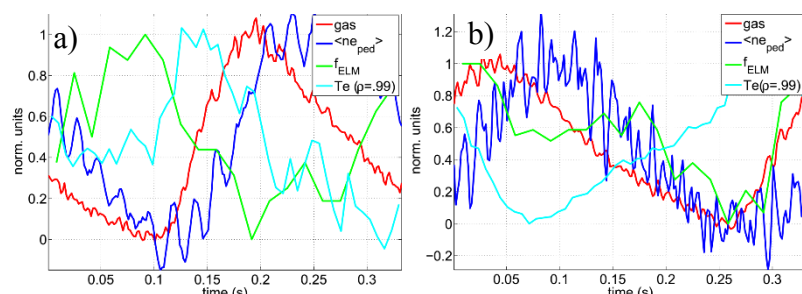


Figure 1 ELM frequency versus gas injection, line averaged electron density at the pedestal and electron temperature inside the separatrix coherently averaged over the modulation cycle. All quantities are normalised to allow comparison of the temporal behaviour. Electron temperature and density modulations result in approximately constant pressure over the modulation cycle. a) $ne_{ped} < 3e19 m^{-3}$ b) $ne_{ped} > 3e19 m^{-3}$

when $n_{\text{ped}} < 3 \times 10^{19} \text{ m}^{-3}$ is also seen within the gas modulation cycle (Figure 1) where coherently averaged data are shown for a single cycle. In addition some information of causalities can be extracted. The gas entry to the vessel is seen with a bolometer measuring the total radiation on a line of sight near the gas valve outlet just outside the separatrix. In several cases the ELM frequency is seen to change just after the gas and before the line averaged pedestal density rises indicating that ELM stability is affected by the gas/density rise close to the separatrix and potentially even on the SOL side. However, this is not a universal observation as in many cases the causality is either less evident or the ELM frequency is seen to follow the pedestal density more closely.

Figure 3 shows typical electron density modulation amplitude profiles from gas puff modulation discharges. The height of the narrow peak near separatrix is seen to correlate quite strongly with the gas modulation amplitude as expected (see Figure 4). The axisymmetric gas injection from divertor locations (gims 9 to 11) are seen to be less efficient in generating the edge peak. However, when plotting the modulated electron density amplitude at $\rho = 0.95$ (see dashed line in Figure 3) which is expected to be of more relevance for core fuelling efficiency all fuelling locations seem equally efficient in generating the density response. The reason for this is not understood. One possibility is that the strong peak at the edge is due to main chamber fuelling while the X-point region would yield spatially more uniform source profile.

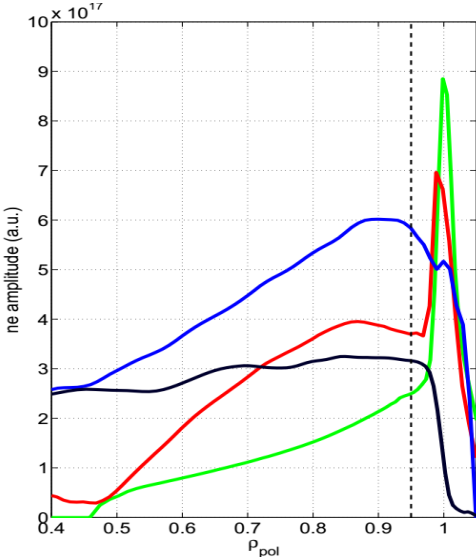


Figure 3 Typical electron density modulation amplitude profiles as measured with reflectometer. Colours are used to better distinguish different shapes and do not refer to any other plots. Only profile shapes (not magnitudes) can be compared with each other.

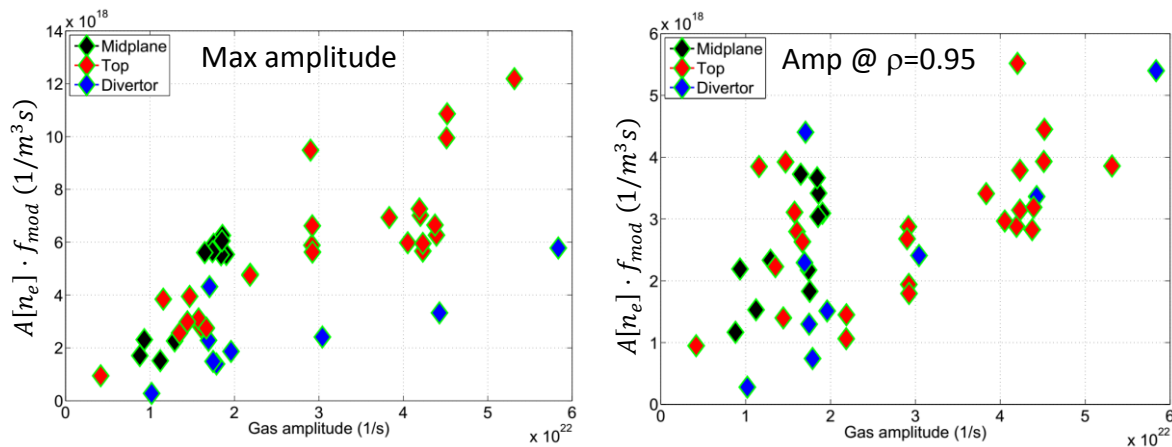


Figure 4 Measured electron density amplitude near separatrix (left) and at $\rho = 0.95$ (right) as a function of gas modulation amplitude. The symbols indicate the gas injection location (gims 9 to 11 are at the divertor, 1&4 at LFS midplane and 7&8 at the top).

Figure 5 shows the normalised electron density modulation as a function of pedestal transparency

$\Delta_{CX} = (S_{CX}/3S_i)^{1/2} \lambda_{CX}$ where $\lambda_{CX} = v_{th}/(nS_{CX})$, here v_{th} is the ion thermal speed, n is the electron density and S_{CX} and S_i are the charge exchange and ionization cross sections, respectively [2]. We can see that there is no clear trend. In L-mode both the density and

temperature pedestals are low leading to long neutral mean free path. The normalized electron density modulation inside the pedestal is somewhat larger than in H-modes but there is no clear trend. The H-mode plasmas only span a factor of 2 in the pedestal transparency parameter (from 0.04 to 0.08) and show very little correlation between the transparency and the response inside the pedestal. One reason for the lack of correlation in H-mode could be the coupling between ELM frequency and the pedestal density and/or gas fuelling (see Figures 1 and 2). Increased particle source from gas puffing could be partially counteracted by the increased losses due to higher ELM frequency. On the other hand, higher ELM frequency tends to come with smaller ELM size so that the particle pump-out may not increase as quickly as the ELM frequency itself.

The delays in the poloidal evolution of radiation, SOL density and ion saturation current suggest that the typical time for the SOL to adjust to the new gas puff/pumping conditions is 20-50ms. Ion saturation current rise after the gas puff is often seen first in the far SOL region (probe 36) potentially indicating a recycling cascade moving towards the separatrix (on ~ 10 ms time scale, see Figure 6).

Strike point sweeping

was used for the first time to generate SOL, pumping and recycling changes while maintaining main plasma shape and keeping all other parameters constant. The goal here was

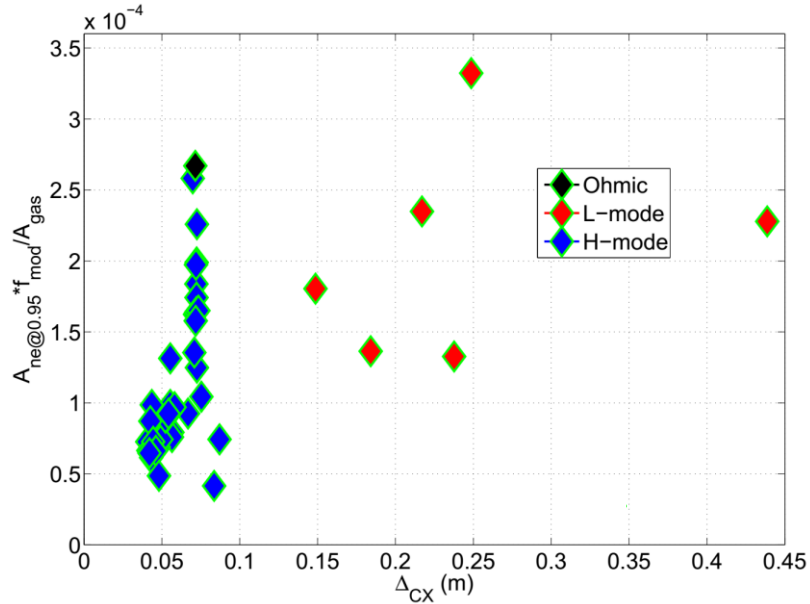


Figure 5 Normalised electron density modulation at $\rho=0.95$ versus pedestal transparency. Legend does not cover any L-mode cases.

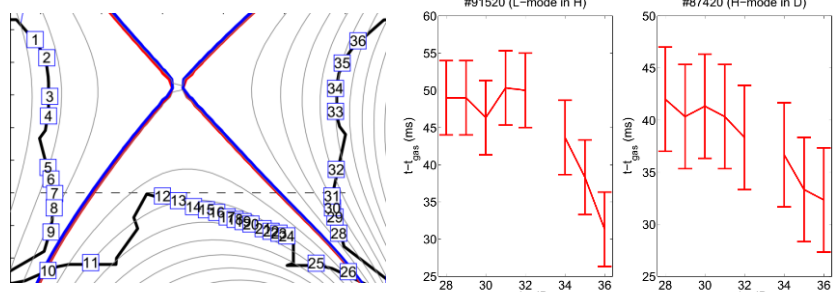


Figure 6 Divertor configuration with Langmuir probe locations indicated with numbers inside square boxes (left) and delay in ion saturation current response on the right hand side vertical target w.r.t. the gas injection from top of the plasma.

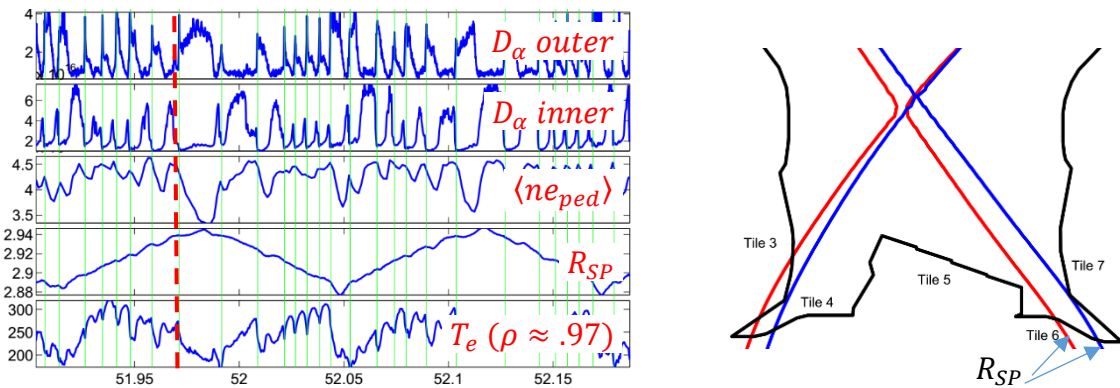


Figure 7 Electron density variation during strike point sweeping. Green vertical lines indicate ELMs occurrences and the dashed red line shows an apparent H-L transition when the strike points gets close to the tile 7. L-H transition occurs as quickly as the strike point returns on the horizontal tile 6. The reduction of the inner divertor D_{α} radiation during an ELM is an indication of inner strike point detachment.

to find a scheme that could be used to create a fast modulation of SOL particle source to allow capturing it from the measured electron density response. Indeed, a strong effect on electron density in the confined plasma and in ELM frequency was seen when the outer strike point was being swept on tiles 5 or 6. Sweeping on the vertical tile 7 was limited in practice to ~ 2 cm in its extent and no density modulation could be observed outside the measurement error. The interpretation of the sweeps on tile 6 is complicated by the apparent H-L-H transition when the strike point gets close to tile 7 (see e.g. $t=51.97$ s in Figure 7). The higher L-H threshold in vertical configuration seems to be consistent with [1] where radial electric field changes are observed in modelling which are consistent with experiments. The analysis of the sweeping effects on tile 5 is still ongoing; here the strong electron density modulation is not causing L-H transitions thus being potentially useful for edge fuelling studies. However, some puzzling observations such as the electron density modulation amplitudes being nearly the same at 4, 8 and 18.5 Hz sweeping frequencies in otherwise identical conditions may indicate problems in equilibrium reconstruction that still need to be carefully analysed.

In addition to what was shown above, we have observed that the plasma fuelling dynamics are quite complicated, and it has not yet been possible to draw a uniform picture of the process from the measurements alone. The question of fuelling is obviously important to understand and we are working, e.g. on integrated core-edge-SOL modelling of the modulated gas fuelling to gain more insight of the various contributions. The dynamical information such as shown in Figures 2 and 6 is hoped to constrain the modelling sufficiently for quantitative interpretation.

[1] A. Chankin et al, EDGE2D-EIRENE modelling of near SOL, to be published in PPCF, 2017

[2] M.F.A Harrison, Physics of Plasma-Wall Interactions in Controlled Fusion, Plenum Press, New York, 1986

This work has been carried out within the framework of the EUROfusion Consortium and has received funding from the Euratom research and training programme 2014-2018 under grant agreement No 633053. The views and opinions expressed herein do not necessarily reflect those of the European Commission